Asian Journal of Basic Science & Research
Volume 6, Issue 1, Pages 142-153, January-March 2024

# Hydrocarbon Play Assessment in Fuba Field, Onshore Niger Delta, Nigeria

U. Ochoma[1*]

[1]*Department of Physics, Rivers State University, P.M.B 5080, Port Harcourt, Nigeria.*
*Corresponding Author Email: umaocho@gmail.com**

*DOI: http://doi.org/10.38177/AJBSR.2024.6113*



*Article Received: 29 December 2023* *Article Accepted: 27 February 2024* *Article Published: 25 March 2024*

ABSTRACT

Hydrocarbon Play Assessment in Fuba Field, Onshore Niger Delta, Nigeria, are here presented, using 3D seismic and well log data. Two distinct horizons (A and I) were correlated across all seven wells in the field. The two reservoir sand units were evaluated quantitatively for petrophysical properties such as shale volume, total porosity, effective porosity, net-to-gross (NTG) and water saturation. Shale volume values have a range of 8 to 14% in reservoir A and 10 to 25% in reservoir I. Porosity values have a range of 25.00 to 30.00% in reservoir A and 19.00 to 37.00% in reservoir I. NTG values have a range of 86.00 to 92.00% in reservoir A and 75.00 to 90.00% in reservoir I, water saturation values have a range of 10.00 to 41.00% in reservoir A and 11.00 to 54.00% in reservoir I. Structural interpretation of seismic data revealed that the field is highly faulted with synthetic and antithetic faults which are in line with faults trends identified in the Niger Delta. A total of twenty-nine faults were interpreted across the entire seismic data. Fault and horizon interpretation revealed that closures found on A and I reservoirs are collapsed crestal structures bounded by two major faults. The depth structure maps reveal that the reservoirs are anticlinal and fault supported. Reservoir A is found at a shallower depth from 6500 to 7500 ft while reservoir I is found at a depth ranging from 11500 to 13000 ft. The seismic attributes interpreted include variance edge and chaos. The variance edge and chaos attribute values range from 0.00 to 1.00. They revealed the subtle structures and faults in the seismic section. The trapping mechanism of the field is of both anticlinal and fault-assisted closure also, the viability of the reservoir units is high from the computed petrophysical parameters.

**Keywords:** Well logs; Porosity; Permeability; Growth faults; Niger Delta; Nigeria.

## 1.0. Introduction

Hydrocarbon play assessment of any hydrocarbon reservoir unit depends on the porosity, permeability, hydrocarbon saturation, water saturation and seismic reflections of reservoir rocks (Ibe and Oyewole, 2019). Estimation of the structural and petrophysical evaluation of every reservoir unit require the integration of seismic and well log data, to describe the reservoir properties in terms of thickness, subsurface structural traps, porosity, permeability, hydrocarbon saturation, etc., within a particular field (Mehdipour et al., 2003). Evaluation of the trapping styles is fundamental in the analysis of a prospect and an essential part in any successful oil and gas exploration program or resource assessment program (Oyeyemi and Aizebeokhai, 2015; Emujakporue, 2016). Core samples and well logs can be used to determine or estimate the petrophysical properties, also sonic, neutron or bulk density log can be used to obtain the porosity value; hence, resistivity logs contribute to calculating the water saturation and fluid discrimination of the reservoir units (Emujakporue, 2017). Stochastic and deterministic modeling are the two methods that can also evaluate the reservoir property, and it is always difficult to obtain the spatial distribution of the petrophysical properties using the deterministic approach as it requires the inverse distance weighting method and it assumes a single value at a point (Miller et al., 2000; Adeoti et al., 2014; Qihong et al., 2000). Several researchers have made enormous contributions based on hydrocarbon play assessment within the Niger Delta basin to investigate the potentiality of hydrocarbon deposits (Ochoma et al., 2020; Kataike et al., 2016; Fajana et al., 2018). Kataike et al., (2016) used gravity and magnetic data to estimate the average thickness of the sediments within the Semliki Basin, to identify the fault systems around the Turaco Prospect and to identify basement controlled sedimentary structures within the Semliki Basin. The gravity data revealed a depocenter of approximately 5km which implied that the sediments were thick enough to generate hydrocarbons. The derivatives

disclosed fault structures with the main faults being the Kibuku, Makondo, Toro-Bunyoro and Semliki faults. Using the Euler deconvolution, an average thickness of sediments in the range of 2-5km was observed. Forward modeling revealed that the Turaco structure is fault controlled and therefore, the identified faults could be the potential traps for the Turaco prospect. It can therefore, be concluded that the main structures which could possibly be potential hydrocarbon traps in the study area are probably fault controlled. Fajana et al., (2018) integrated seismic interpretation and petrophysical assessment of borehole logs from seven wells were with the aim of establishing the hydrocarbon reserves prior to field development which will involve huge monetary obligation. Four horizons corresponding to near top of mapped hydrocarbon-bearing sands were used to produce time maps and then depth structural maps using checkshot data. Three major structure-building faults (F2, F3 and F5 which are normal, listric concave in nature) and two antithetic (F1 and F4) were identified. Structural closures identified as rollover anticlines and displayed on the time/depth structure maps suggest probable hydrocarbon accumulation at the upthrown side of the fault F4. Petrophysical analysis of the mapped reservoirs showed that the reservoirs are of good quality and are characterized with hydrocarbon saturation ranging from 56 to 72%, volume of shale between 7 and 20% and porosity between 25 and 31%. This research study revealed that the discovered hydrocarbon reserve resource accumulations in the Pennay field for the four-mapped reservoir sand bodies have a total proven (1P) reserve resource estimate of 53.005MMBO at P90, 59.013MMBO at 2P/P50 and 65.898MMBO at 3P/P10. Reservoir C, the only interval with a gas cap, has a volume of 7737MMscf of free gas at 1P, 8893.2MMscf at 2P and 10185.2MMscf at 3P. These oil and gas volumetric values yield at 1P/ P90 total of 137.30MMBOE, 154.9MMBOE at 2P and 171.515MMBOE at 3P. Reservoirs B and D have the highest recoverable oil at 1P, 2P, and 3P values of 5.265MMBO and 10.70MMBO, 12.053MMBO and 5.783MMBO, 13.557MMBO and 6.244MMBO, respectively.

This study is taken from Fuba Field, Depobelt, Niger Delta, Nigeria. The ultimate deliverable of this study was hydrocarbon play assessment of the area. The major components of this study are: (a) Well Correlation performed in order to determine the continuity of the reservoir sand across the field. (b) Petrophysical evaluation. (c) Seismic Interpretation which involves well-to-seismic ties, fault mapping, horizon mapping, time surface generation, depth conversion and attributes generation. This gives more insight into hydrocarbon play assessment of the area.

## 2.0. Location and Geology of the Study Area

The proposed study area Fuba Field is located in the onshore Niger Delta region. Figure 1 shows the map of the Niger Delta region showing the study area while Figure 2 shows the base map showing well locations in the study area. The Niger Delta lies between latitudes 4° N and 6° N and longitudes 3° E and 9° E (Whiteman, 1982). The Delta ranks as one of the major oil and gas provinces globally, with an estimated ultimate recovery of 40 billion barrels of oil and 40 trillion cubic feet of gas (Adegoke et al., 2017). The coastal sedimentary basin of Nigeria has been the scene of three depositional cycles (Short and Stauble, 1967).

The first began with a marine incursion in the middle Cretaceous and was terminated by a mild folding phase in Santonian time. The second included the growth of a proto-Niger delta during the Late Cretaceous and ended in a major Paleocene marine transgression. The third cycle, from Eocene to Recent, marked the continuous growth of the main Niger delta. A new threefold lithostratigraphic subdivision is introduced for the Niger delta subsurface,

Asian Journal of Basic Science & Research
Volume 6, Issue 1, Pages 142-153, January-March 2024

comprising an upper sandy Benin Formation, an intervening unit of alternating sandstone and shale named the Agbada Formation, and a lower shaly Akata Formation. These three units extend across the whole delta and each ranges in age from early Tertiary to Recent. They are related to the present outcrops and environments of deposition. A separate member of the Benin Formation is recognized in the Port Harcourt area.

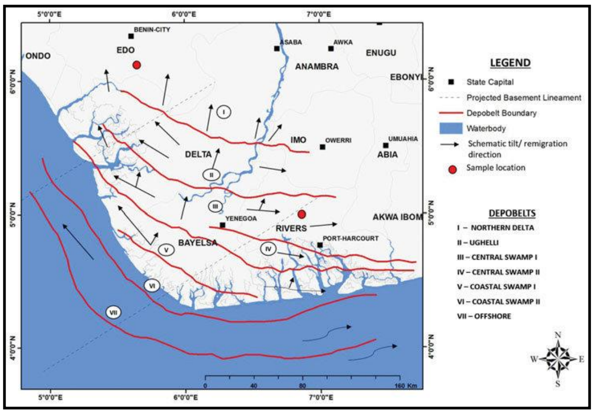


**Figure 1.** Map of Niger Delta Showing the study Area

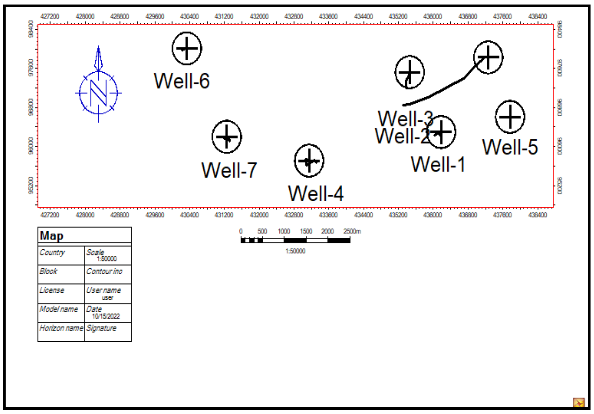


**Figure 2.** Base Map of Showing Well Locations in the Study Area

It is Miocene-Recent in age with a minimum thickness of more than 6,000ft (1829m) and made up of continental sands and sandstones (>90%) with few shale intercalations (Horsfall et al., 2017). Subsurface structures are described as resulting from movement under the influence of gravity and their distribution is related to growth stages of the delta (Ochoma et al, 2020). Rollover anticlines in front of growth faults form the main objectives of oil exploration, the hydrocarbons being found in sandstone reservoirs of the Agbada Formation. The oil in geological structures in the basin may be trapped in dip closures or against a synthetic or antithetic fault.

## 3.0. Methodology

### 3.1. Well-Log Data Quality Control

Well correlation involves lithologic description, picking top and base of sand-bodies, fluid discrimination and then linking these properties from one well to another based on similarity in trends. Correlation of reservoir sands was achieved using the top and base of reservoir sands picked. The correlation process was possible based on similarity in the behaviour of the gamma ray log. In the Niger Delta, the predominant lithologies are sands and shales. In order to discriminate between these two lithologies in the subsurface, the gamma ray log is used. After defining the lithologies, the resistivity log was used for discriminating the type of fluid occurring within the pores in the rocks.

### 3.2. Petrophysical Evaluation

#### 3.2.1. Shale Volume ($V_{SH}$)

This is the space occupied by shale or the fraction of shale (clay), present in reservoir rock (Cannon, 2018). The volume of shale is determined from mathematical correlations and gamma ray index. In mathematical equations, the volume of shale is represented as $V_{SH}$. The gamma ray index ($GR_{index}$) was first calculated in order to calculate the shale volume based on Schlumberger (1974) empirical equation as follows;

$$GR_{index} = \frac{GR_{\log} - GR_{min}}{GR_{\max} - GR_{min}} \qquad (1)$$

Where;

$GR_{\log} = GR$ log reading of formation

$GR_{min} = GR$ sand baseline

$GR_{\max} = GR$ shale baseline

The Larionov (1969) equation for tertiary reservoirs was utilized for calculating the shale volume as follows;

$$V_{sh} = 0.083 \times (2^{(3.7 \times GR_{index})} - 1) \qquad (2)$$

### 3.2.2. Effective Porosity

The effective porosity is the porosity that is responsible for flow to occur within the reservoir. Effective porosity ($\Phi_E$) was calculated using volume of shale (Vsh) and total porosity ($\Phi_T$) as follows (Dresser, 1979);

$$\phi_E = (1 - V_{sh}) \times \phi_T \qquad (3)$$

Where;

$\phi_E =$ Effective porosity

$\phi_T =$ Total porosity

$V_{sh} =$ Volume of shale

### 3.2.3. Net to Gross

The net-to-gross ratio reduces the maximum reservoir thickness to the anticipated pay (permeable reservoir) thickness. Net-to-Gross sand is reservoir thickness less shale thickness. This is a factor used to identify probable producing regions of a formation. To determine the clean sand content, Net to Gross was calculated as follows;

$$Net - to - gross = \frac{NH}{GH} \qquad (4)$$

Where;

$NH =$ Net thickness

$GH =$ Gross thickness

### 3.2.4. Water Saturation

This is the relative extent to which the pores in rocks are filled with water. Saturation is expressed as the fraction, or percent, of the total pore volume occupied by the oil, gas, or water. Water saturation is denoted as $S_w$ and is

expresses in percent or fraction. Water saturation is predominantly controlled by porosity and formation resistivity. It can be calculated using Archie (1942) empirical model as follows;

$$S_w = \left(\frac{a \times R_w}{R_t \times \phi_t^m}\right)^{\frac{1}{n}} \qquad (5)$$

Where;

$S_w =$ Archie's water saturation for clean sand

$a =$ tortuosity factor = 1

$m =$ cementation exponent = 2

$n =$ saturation exponent = 2

$R_t =$ formation resistivity (read from log)

$R_w =$ formation water resistivity (read from log)

$\phi_t =$ total porosity

### 3.3. Seismic Interpretation

There are six basic steps involved in seismic interpretation relevant to this study and they include well-to-seismic ties, fault mapping, horizon mapping, time surface generation, depth conversion and attributes generation. The sonic log, which is the reciprocal of velocity, was calibrated using the checkshot data. The calibration process is necessary in order to improve the quality of the sonic log because the sonic log is prone to washouts and other wellbore related issues. The results of calibrating the sonic log with the checkshot gives the calibrated sonic log.

The calibrated sonic log is used along with the density log to generate an acoustic impedance (AI) log. The acoustic impedance log is calculated for each layer of rock. The next step involves generating the reflectivity coefficient (RC) log. The RC is calculated and generated using the AI log. The RC log generated is then convolved with a wavelet to generate a synthetic seismogram which is comparable with the seismic data. The statistical wavelet utilized for convolution is extracted from the seismic data. The synthetic seismogram was generated. The mathematical expressions that govern the entire well-to-seismic tie workflow are presented below:

$$AI = \rho v \qquad (6)$$

$$RC = \frac{\rho_2 v_2 - \rho_1 v_1}{\rho_2 v_2 + \rho_1 v_1} \qquad (7)$$

$$\text{Synthetic Seismogram} = \frac{\rho_2 v_2 - \rho_1 v_1}{\rho_2 v_2 + \rho_1 v_1} * wavelet \qquad (8)$$

where AI = acoustic impedance, RC = reflection coefficient, ρ = density; v = velocity.

Faults were identified as discontinuities or breaks in the seismic reflections. Faults were mapped on both inline and cross-line directions. Horizons are continuous lateral reflection events that are truncated by fault lines. The horizon interpretation process was conducted along both inline and crossline direction. At the end of the horizon mapping, a seed grid is generated which serves as an input for time surface generation. Time surfaces were generated using the

Asian Journal of Basic Science & Research
Volume 6, Issue 1, Pages 142-153, January-March 2024

seed grids gotten from the horizon mapping process. The third order polynomial velocity model generated was used to depth convert the time surfaces of the reservoirs of interest.

### 3.3.1. Variance (Edge Detection) Method

The variance attribute is edge imaging and detection techniques. It is used for imaging discontinuity related to faulting or stratigraphy in seismic data. Variance attribute is proven to help in imaging of channels, fault zones, fractures, unconformities and the major sequence boundaries (Pigott et al., 2013). In the Petrel software, the variance attribute uses an algorithm that computes the local variance of the seismic data through a multi-trace window with user-defined size. The local variance is computed from horizontal sub-slices for each voxel. A vertical window was used for smoothing the computed variance and the observed amplitude normalized. The variance attribute measures the horizontal continuity of the amplitude that is the amplitude difference of the individual traces from their mean value within a gliding CMP window.

$$\sigma^2 = \frac{1}{n}\sum_{f_i=1}^{n}(x_i + x_m)^2 \qquad (9)$$

Where $\sigma =$ standard deviation, $\sigma^2 =$ variance, $n =$ the number of observations, $f_i =$ frequency

$x_i =$ the variable, $x_m =$ mean of $x_i$

### 3.3.2. Chaos

Chaos attribute is defined as a measure of the “lack of organization” in the dip and azimuth estimation method. It can be used to distinguish different sediment facies in lithology variation environments (for example, sand and shale).

## 4.0. Results and Discussion

### 4.1. Reservoir Identification, Correlation and Well-to-Seismic Ties

The results for lithology and reservoir identification are presented in (Figure 3). A total of nine sand bodies (A, B, C D, E, F, G, H and I) were identified and correlated across all seven wells in the field. Two reservoir sands were selected for the purpose of this study (A and I). The resistivity logs which reveals the presence of hydrocarbons were used to identify the hydrocarbon bearing sands. On (Figure 3), the sands are coloured yellow while shales are black in colour. A statistical wavelet (ISIS) was used to give a near perfect match between the seismic and synthetic seismogram.

### 4.2. Petrophysical Evaluation

The two reservoir sand units were evaluated quantitatively for petrophysical properties such as shale volume, total porosity, effective porosity, net-to-gross (NTG) and water saturation. The summary of these estimated attributes towards formation evaluation analysis are presented in Tables 1 and 2. Shale volume values have a range of 8 to 14% in reservoir A and 10 to 25% in reservoir I. Porosity values have a range of 25.00 to 30.00% in reservoir A and 19.00 to 37.00% in reservoir I. Rider (1986) classified reservoirs having porosity ranging between 20-30% as very good quality reservoirs. Based on this classification, reservoir A and I are classed as very good quality. NTG is 86.00 to 92.00% in reservoir A and 75.00 to 90.00% in reservoir I, water saturation is 10.00 to 41.00% in reservoir

A and 11.00 to 54.00% in reservoir I. Figure 4 compares the petrophysical parameters for both mapped reservoirs. The results of these petrophysical attributes analysis revealed the presence of hydrocarbon in the two correlated reservoir sand units at quantities favourable for commercial exploitation. The high values of the estimated porosity denote that the reservoir sand units are well sorted. The variations in the porosity of the reservoir units across the Niger Delta basin could be ascribed to the differential volume of shale in the reservoirs. The evaluated petrophysical parameters are in line with that of other researchers (Olowokere and Ojo, 2011; Aigbedion and Aigbedion, 2011). These petrophysical properties obtained are the parameters required for estimating the hydrocarbon in place.

### 4.3. Faults and Horizons Interpretation

The results for the interpreted faults in Fuba field are presented in Figure 5 shows both synthetic and antithetic faults interpreted along seismic inlines. Faults are more visible along the inline direction because this direction reveals the true dip position of geologic structures. The variance time slice was used to validate the interpreted faults as seen on Figure 6. All interpreted faults are normal synthetic and antithetic faults. A total of twenty-nine faults were interpreted across the entire seismic data. Of the 29 interpreted faults, only F1 (synthetic fault) and F16 (antithetic fault) faults are regional, running from the top to bottom across the field. Hence, these faults play significant roles in trap formation at the upper, middle and lower sections of the field. The results for the interpreted seismic horizons (Horizon A and Horizon I) are also presented in Figure 5. On these horizons, the fault polygons were generated and eliminated. The horizons were used as inputs for the generation of reservoir time surfaces.

The reservoir time surfaces (A and I reservoirs) reveal that the reservoir structure is a collapsed crest, bounded by two regional faults (F1 and F4). Reservoir A and I time surfaces are truncated by two bounding faults and three minor inter-reservoir faults. The similarity in structure identified on reservoirs A and I reveals that the field is structurally controlled by faults. Figure 7 shows the 3$^{rd}$ order polynomial velocity model which was used as most suitable velocity model for converting A and I reservoirs from time to depth. The depth converted reservoir A and I surfaces are presented in Figures 8 and 9 for the third order polynomial velocity function. The depth structure maps reveal that the reservoirs are anticlinal and fault supported. Reservoir A is found at a shallower depth from 6500 to 7500 ft while reservoir I is found at a deeper depth ranging from 11500 to 13000 ft respectively.

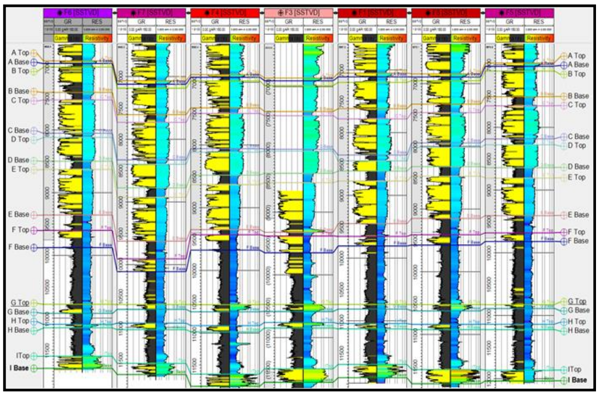

**Figure 3.** Well Section Showing Reservoir Identified and Correlated Across Fuba Field

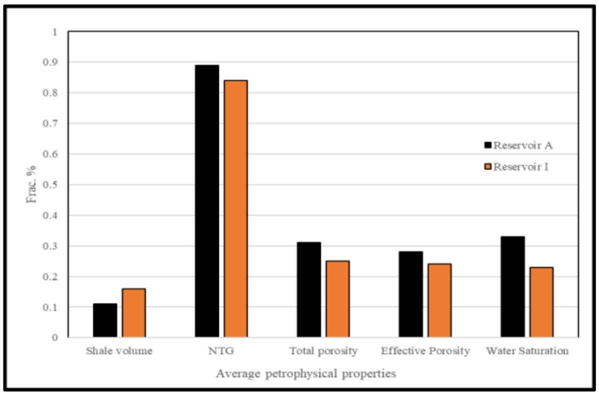


**Figure 4.** Histogram Showing Average Petrophysical Values For A and I Reservoirs

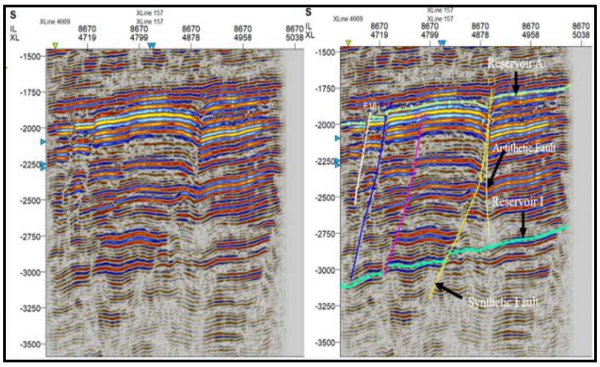


**Figure 5.** Faults and Horizons Interpreted Along Seismic Inline

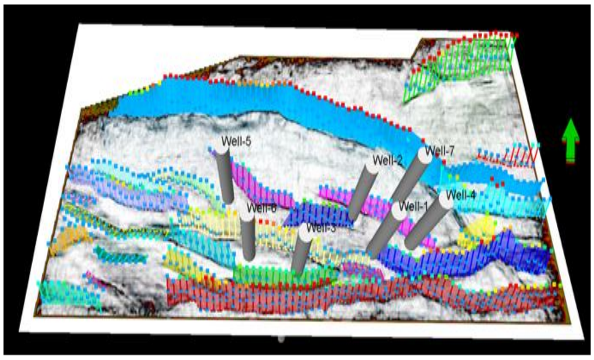


**Figure 6.** Interpreted Faults Displayed on Variance Time Slice

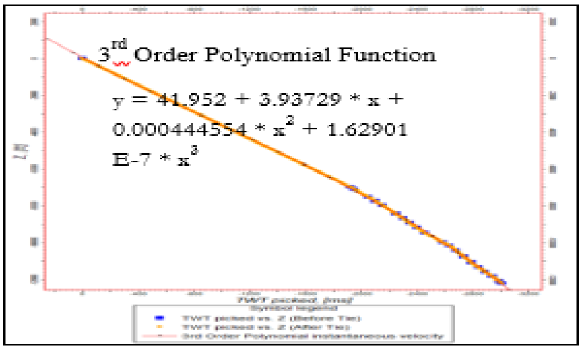


**Figure 7.** Third Order Polynomial Velocity model Utilized for Converting Reservoir Surfaces from Time to Depth Function

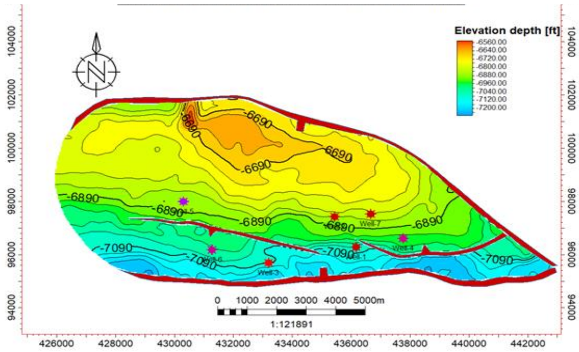


**Figure 8.** Depth Converted Reservoir Surfaces Using the 3rd Order Polynomial Velocity for Reservoir A

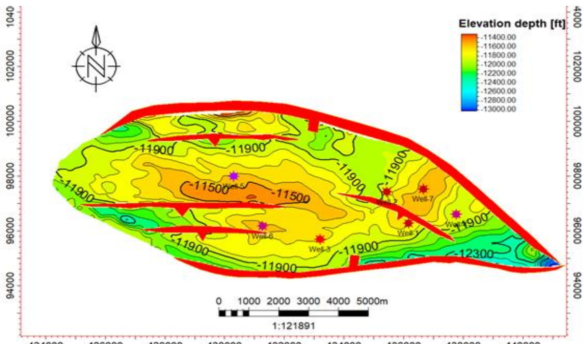


**Figure 9.** Depth Converted Reservoir Surfaces using the 3rd Order Velocity function for Reservoir I

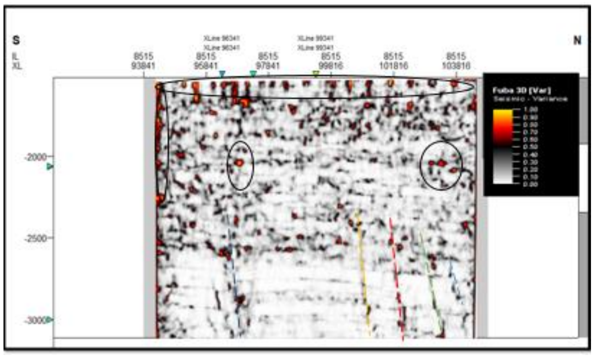

**Figure 10.** Variance Edge inline 8515

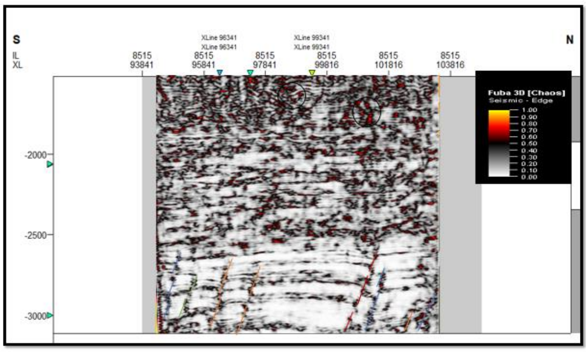

**Figure 11.** Chaos inline 8515

Asian Journal of Basic Science & Research
Volume 6, Issue 1, Pages 142-153, January-March 2024

### 4.4. Seismic Attributes

Variance edge and chaos attributes were generated in Petrel software interface to investigate potential structural and stratigraphic controls within the study area.

Figures 10 and 11 show the computed variance and chaos attributes of the seismic section. The variance and chaos values range from 0.0 to 1.0. Values of variance equal to 1 represent discontinuities while a continuous seismic event is represented by the value of 0. The high values are denoted with red to yellow colorations. On the variance and chaos maps, the areas dotted with blue, green, orange and pink colored lines signify values that correspond to the location of the discontinuity. The discontinuities may be interpreted as faults and boundaries as shown by the lines drawn on the attribute map (Law and Chung, 2006). The variance edge and chaos enhanced the faults or sedimentological bodies within the seismic data volume. Furthermore, several bright spots are also delineated (in black circles and black ovals) which indicate high reflectivity sediments compared to their surroundings. These bright spots are an indication that a potential hydrocarbon trap might exist in the area. The darkest regions in the seismic section, which make vertical strips, may be interpreted as faults or fractures. The zones with low variance values are due to similar seismic traces. Areas with red patches represent lineaments/discontinuities while grey areas represent the structural framework of the field.

**Table 1.** Results of Petrophysical Evaluation for Reservoir A

| Wells | Reservoir Top (MD ft) | Reservoir Base (MD ft) | Gross thickness (ft) | Shale volume (%) | Net thickness (ft) | NTG (%) | Effective Porosity (%) | Water Saturation (%) |
|---|---|---|---|---|---|---|---|---|
| Well-3 | 6930.00 | 6980.00 | 50.00 | 10.00 | 45.00 | 90.00 | - | 37.00 |
| Well-5 | 6957.00 | 7011.00 | 54.00 | 11.00 | 48.06 | 89.00 | - | 41.00 |
| Well-6 | 7101.00 | 7170.00 | 69.00 | 8.00 | 63.48 | 92.00 | - | 40.00 |
| Well-7 | 6910.00 | 6959.00 | 49.00 | 14.00 | 42.14 | 86.00 | - | 33.00 |
| Well-1 | 7091.00 | 7150.00 | 59.00 | 11.00 | 52.51 | 89.00 | 30.00 | 38.00 |
| Well-4 | 7024.00 | 7078.00 | 54.00 | 14.00 | 46.44 | 86.00 | 25.00 | 33.00 |
| Well-2 | 6861.00 | 6920.00 | 59.00 | - | - | - | - | 10.00 |
| Averages | | | 56.29 | 11.00 | 49.61 | 89.00 | 28.00 | 33.00 |

**Table 2.** Results of Petrophysical Evaluation for Reservoir I

| Wells | Reservoir Top (MD ft) | Reservoir Base (MD ft) | Gross thickness (ft) | Shale volume (%) | Net thickness (ft) | NTG (%) | Effective Porosity (%) | Water Saturation (%) |
|---|---|---|---|---|---|---|---|---|
| Well-1 | 11745.00 | 11962.00 | 217.00 | 22.00 | 169.26 | 78.00 | 21.00 | 18.00 |
| Well-2 | 11484.00 | 11735.00 | 251.00 | 10.00 | 225.90 | 90.00 | - | 11.00 |
| Well-3 | 11717.00 | 11900.00 | 183.00 | 15.00 | 155.55 | 85.00 | 20.00 | 19.00 |
| Well-4 | 11925.00 | 12084.00 | 159.00 | 12.00 | 139.92 | 88.00 | 24.00 | 54.00 |
| Well-5 | 11652.00 | 11842.00 | 190.00 | 18.00 | 155.80 | 82.00 | 22.00 | 21.00 |
| Well-6 | 11611.00 | 11788.00 | 177.00 | 25.00 | 132.75 | 75.00 | 19.00 | 23.00 |
| Well-7 | 12000.00 | 12240.00 | 240.00 | 13.00 | 208.80 | 87.00 | 37.00 | 15.00 |
| Averages | | | 202.43 | 16.00 | 169.71 | 84.00 | 24.00 | 23.00 |

## 5.0. Conclusion

A total of nine sand bodies (A, B, C D, E, F, G, H and I) were identified and correlated across all seven wells in the field. Two horizons (A and I) were selected for the study. The two reservoir sand units were evaluated quantitatively for petrophysical properties such as shale volume, total porosity, effective porosity, net-to-gross (NTG) and water saturation. Shale volume values have a range of 8 to 14% in reservoir A and 10 to 25% in reservoir I. Porosity values have a range of 25.00 to 30.00% in reservoir A and 19.00 to 37.00% in reservoir I. Rider (1986) classified reservoirs having porosity ranging between 20-30% as very good quality reservoirs. Based on this classification, reservoir A and I are classed as very good quality. NTG values have a range of 86.00 to 92.00% in reservoir A and 75.00 to 90.00% in reservoir I, water saturation values have a range of 10.00 to 41.00% in reservoir A and 11.00 to 54.00% in reservoir I. Structural analysis of the field revealed that reservoir A and I are anticlinal structures supported by two major bounding faults. Structural interpretation of seismic data revealed that the field is highly faulted with synthetic and antithetic faults which are in line with faults trends identified in the Niger Delta. All interpreted faults are normal synthetic and antithetic faults. A total of twenty-nine faults were interpreted across the entire seismic data. Of the 29 interpreted faults, only F1 (synthetic fault) and F16 (antithetic fault) faults are regional, running from the top to bottom across the field. Hence, these faults play significant roles in trap formation at the upper, middle and lower sections of the field. Fault and horizon interpretation revealed that closures found on A and I reservoirs are collapsed crestal structures bounded by the two major faults. The depth structure maps reveal that the reservoirs are anticlinal and fault supported. Reservoir A is found at a shallower depth from 6500 to 7500 ft while reservoir I is found at a depth ranging from 11500 to 13000 ft respectively. The seismic attributes interpreted include variance edge and chaos. The variance edge and chaos attribute values range from 0.00 to 1.00. They revealed the subtle structures and faults in the seismic section. Finally, it is recommended that recommended that further studies should include biostratigraphy data of all the wells. This will provide more reliable data for further interpretation of the field. Integrated studies such as drill stem test, repeat formation test results and engineering data should be added to the results of this study to further ascertain the fluid types identified in the wells and also give evidence that reservoir fluid is actually recoverable. These will contribute significantly to the efficient development of the hydrocarbon in the study area.

**Declarations**

**Source of Funding**

This study did not receive any grant from funding agencies in the public, commercial, or not-for-profit sectors.

**Competing Interests Statement**

The author declares no competing financial, professional, or personal interests.

**Consent for publication**

The author declares that she consented to the publication of this study.

**Acknowledgements**

The author is grateful to Shell Petroleum Development Company of Nigeria (SPDC), Port Harcourt Nigeria for the release of the academic data for the purpose of this study.

**References**

[1] Ibe, A.A., & Oyewole, T.E. (2019). Hydrocarbon Play Assessment of X-field in an Onshore Niger Delta, Nigeria. Journal of Petroleum Exploration and Production Technology, 9: 61–74.

[2] Mehdipour, V., Ziaee, B., & Motiei, H. (2003). Determination and Distribution of Petrophysical Parameters (PHIE, Sw and NTG) of Ilam Reservoir in One Iranian Oil field. Life Science Journal, 10: 153–161.

[3] Oyeyemi, D.K., & Aizebeokhai, P.A. (2015). Hydrocarbon Trapping Mechanism and Petrophysical Analysis of Afam Field, Offshore Nigeria. International Journal of Physical Sciences, 10(7): 222–238.

[4] Emujakporue, G.O. (2016) Evaluation of Hydrocarbon Prospect of Amu field, Niger Delta, Nigeria. International Research Journal of Geology and Minning, 6(1): 1–8.

[5] Emujaporue, G.O. (2017) Petrophysical Properties Distribution Modeling of an Onshore Field, Niger Delta Nigeria. Current Research in Geoscience, 7(1): 14–24.

[6] Miller, R.B., Castle, J.W., & Temples, T.J. (2000). Deterministic and Stochastic Modeling of Aquifer Stratigraphy, South Carolina. Ground water, 38: 284–195.

[7] Adeoti, L., Onyekachi, N., Olatinsu, O., Fatoba, J., & Bello, M. (2014). Static Reservoir Modeling using Well Log and 3D Seismic Data in a KN Field, Offshore Niger Delta, Nigeria. International Journal of Geoscience, 5: 93–106.

[8] Qihong, L., Zigi, S., & Chengqian, T. (2000). Reservoir Description of the Stochastic Simulation Method. J Xi'an Petroleum Institute, 15: 13–16.

[9] Ochoma, U., Uko, E.D., & Horsfall, O.I. (2020). Deterministic Hydrocarbon Volume Estimation of the Onshore Fuba Field, Niger Delta, Nigeria. IOSR Journal of Applied Geology and Geophysics, 8(1): 34–40.

[10] Kataike, W., Batte, G., & Aanyu, K. (2016). Detection of Potential Hydrocarbon Traps in the Semliki Basin using Gravity and Magnetic Data. Kampala, Uganda, 2nd EAGE Eastern Africa Petroleum Geoscience Forum.

[11] Fajana, O.A., Ayuk, A.M., Enikanselu, A.P., & Oyebamiji, R.A. (2018). Seismic Interpretation and Petrophysical Analysis for Hydrocarbon Resource Evaluation of 'Pennay' Field, Niger Delta. Journal of Petroleum Exploration and Production Technology, 9: 1025–1040.

[12] Whiteman, A. (1982). Nigeria: Its Petroleum Ecology Resources and Potential. London, Graham and Trotman.

[13] Adegoke, O.S., Oyebamiji, A.S., Edet, J.J., Osterloff, P.L., & Ulu, O.K. (2017). Cenozoic Foraminifera and Calcareous Nannofossil Biostratigraphy of the Niger Delta. Elsevier, Cathleen Sether, United States.

[14] Short, K.C., & Stable, A.J. (1967). Outline of Geology of Niger Delta. Bulletin of America Association of Petroleum Geologists, 51(5): 761–779.

[15] Horsfall, O.I., Uko, E.D., Tamunoberetonari I., & Omubo-Pepple, V.B. (2017). Rock-Physics and Seismic-Inversion Based Reservoir Characterization of AKOS FIELD, Coastal Swamp Depobelt, Niger Delta, Nigeria. IOSR Journal of Applied Geology and Geophysics, 5(4): 59–67.

[16] Ochoma, U., Uko, E.D., & Ayanninuola, O.S. (2020). Subsurface Structures of Onshore Fuba Field, Niger-Delta, Nigeria. International Journal of Scientific Research in Physics and Applied Sciences. 8(5): 1–5.

[17] Cannon, S. (2018). Reservoir Modelling: A Practical Guide. John Wiley and Sons, Inc., 111 River Street, Hoboken, NJ 07030, USA.

[18] Schlumberger Well Services (1974). Log Interpretation Charts, Schlumberger Educational Services, New York, 83.

[19] Larionov, V. (1969). Borehole Radiometry: Moscow, U.S.S.R., Nedra.

[20] Dresser, A. (1979). Log Interpretation Charts, Dresser Industries Inc., Houston, Texas: 107

[21] Archie, G.E. (1942). The electrical resistivity log as an aid in determining some reservoir characteristics. Journal of Petroleum Technology, 5: 54–62.

[22] Pigott. J.D., Kang, M.I.H., & Han, H.C. (2013). First Order Seismic Attributes for Clastic Seismic Facies Interpretation: Examples from the East China Sea. Journal of Asian Earth Science, 66: 34–54.

[23] Olowokere, M.T., & Ojo, J.S. (2011). Porosity and Lithology Prediction in Eve Field, Niger Delta, using Compaction Curves and Rock Physics Models. International Journal of Geoscience, 2: 336–372.

[24] Aigbedion, I., & Aigbedion, H.O. (2011). Hydrocarbon Volumetric Analysis using Seismic and Borehole Data over Umoru Field, Niger Delta, Nigeria. International Journal of Geoscience, 2: 179–183.

[25] Law, W.K., & Chung, A.S.C. (2006). Minimal Weighted Local Variance as Edge Detector for Active Contour Models. In Narayanan et al. P.J. (Eds.), LNCS 3851, Pages 622–632.

[26] Rider, M.H. (1986). The Geological Interpretation of Well Logs. John Wiley and sons, Inc., New York.